SACLANTCEN REPORT
serial no: SR- 297

SACLANT UNDERSEA RESEARCH CENTRE REPORT

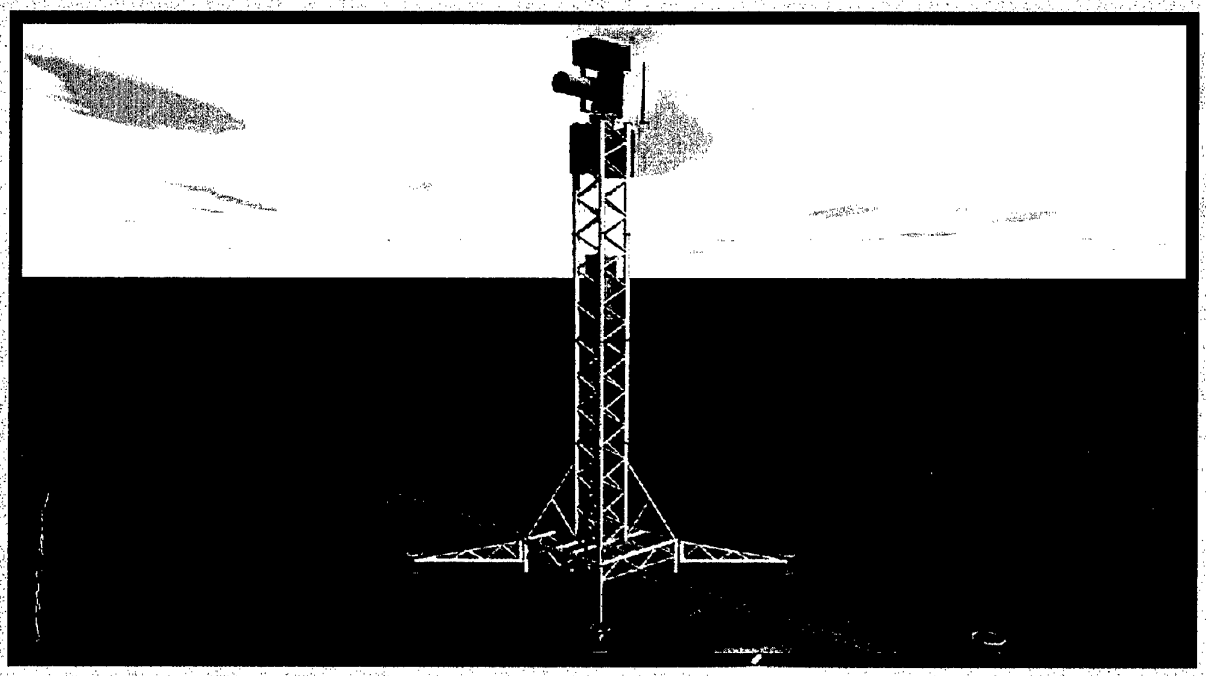

DISTRIBUTION STATEMENT A
Approved for Public Release
Distribution Unlimited

NORTH ATLANTIC TREATY ORGANIZATION ORGANISATION DU TRAITE DE L'ATLANTIQUE NORD

Sediment sound speed and critical angle estimations derived from in situ acoustic measurements

A.Maguer, W.L.J.Fox,
H.Schmidt and E.Bovio

The content of this document pertains to work performed under Project 03A of the SACLANTCEN Programme of Work. The document has been approved for release by The Director, SACLANTCEN.

Jan L. Spoelstra
Director

SACLANTCEN SR-297

intentionally blank page

Sediment sound speed and critical angle estimations derived from in situ acoustic measurements

A.Maguer, W.L.J.Fox, H.Schmidt and E.Bovio

Executive Summary:

Mines which are completely buried in certain types of ocean sediments are considered undetectable by conventional high frequency minehunting sonars. This is due to the very low levels of energy transmitted into the sediment at the low grazing angles used for minehunting. As the attenuative effect of the sediment is reduced at lower frequencies, SACLANTCEN has investigated the possibility of using ower frequency sonar at low grazing angles in order to enhance the ability to hunt buried mines.

A good understanding of the basic physics of sound penetration into the sediment is essential for designing systems that can effectively hunt buried mines. The authors already reported their work about the sub-critical penetration into a sandy bottom. Sound propagation theory can explain the received levels for frequencies below 5-7 kHz, but scattering due to the rough nature of the seabed is the dominant mechanism above these frequencies.

Simulation using Biot theory for different sediment permeability has shown that there may be significant frequency dependence to sediment sound speed and therefore frequency dependence of the critical angle, in the range 1-100 kHz. Sediment sound speed and critical angle estimations were therefore investigated through the analysis of *in situ* acoustic measurements. Acoustic energy in the frequency range 2-16 kHz was directed toward a sandy seabottom where a buried 14-element hydrophone array measured the incoming signals. The sound speed and the critical angle are estimated by analyzing the variations of signal arrival times *versus* frequency, burial depth, and grazing angle. A good match was obtained between the data and the theory. It was found that the sound speed in the sand which better matches the acoustic data in the frequency range 2–5 kHz is equal to 1626 m/s, implying a critical angle on the order of 21°. This value of sound speed in the sandy bottom is quite different to the 1720 m/s sound speed estimated from cores using pulsed sound at 200 kHz, and is in good agreemeent with the Biot theory.

Future work in this area will verify results presented in this report, and generalize them for other types of seabeds. Buried-target backscattering measurements in the same frequency range will be reported. Recommendations for system concepts to enhance the ability to hunt buried mines will be made.

intentionally blank page

Sediment sound speed and critical angle estimations derived from in situ acoustic measurements

A.Maguer, W.L.J.Fox, H.Schmidt and E.Bovio

Abstract:

Understanding the basic physics of sound penetration into ocean sediments is essential to the design of sonar systems which can detect, localize, classify, and identify buried objects. The sediment sound speed is a crucial parameter as the ratio of sound speed at the water-sediment interface determines the critical angle. Sediment sound speed is typically measured from core samples using high frequency (100's of kHz) pulsed travel time measurements. Earlier work on subcritical penetration into sandy sediments has suggested that the effective sound speed in the 2-20 kHz range is significantly lower than the core measurement results. Simulation using Biot theory for propagation in porous media confirmed that sandy sediments may be highly dispersive in the range 1-100 kHz. It is shown that a direct and robust estimate of the critical angle and therefore the sediment sound speed, at lower frequencies can be achieved by analyzing the grazing angle dependence of the phase delays observed on a buried array.

A parametric source with secondary frequencies in the 2-16 kHz range was directed toward a sandy bottom similar to the one investigated in the earlier study. An array of 14 hydrophones was used to measure penetrated field. The critical angle were estimated by analyzing the variations of signal arrival times *versus* frequency, burial depth, and grazing angle. Matching the results with classical transmission theory yielded a sound speed estimate in the sand of 1626 m/s in the frequency range 2–5 kHz, significantly lower than the 1720 m/s estimated from the cores at 200 kHz. This dispersion is consistent with Biot theory.

Keywords: seafloor ∘ scattering ∘ sound penetration ∘ kirchhoff ∘ small perturbation ∘ evanescent wave ∘ Biot theory ∘

Contents

1
INTRODUCTION

In certain types of ocean sediments completely buried mines are considered undetectable by conventional high frequency mine hunting sonars. This is due to the very low level of energy transmitted into the sediment for these frequencies at the low grazing angles used for mine hunting operations. As the attenuative effect of sediment is less at lower frequencies, the possibility of using lower frequency sonars, at low grazing angles, in order to enhance the ability to hunt buried mines has been investigated.

The authors have previously reported an investigation of the mechanisms by which "anomalously" high levels of energy are transmitted into the sediment [1] in the 2–16 kHz regime. The conclusion was that classical sound propagation theory can explain the received levels for frequencies below 5–7 kHz and that scattering due to seabed roughness is the dominant mechanism above these frequencies. However, to match model predictions with penetration data, it was necessary to assume a sound speed which was significantly lower than the one measured on cores at higher frequencies.

As sediment sound speed determines the critical angle, this dispersion is critical to the performance of sonars for buried mine detection. Moreover, the estimation of the sound speed in the sediment is essential for new buried mine classification concepts based on physical scattering models. Thus, a sound speed mismatch may lead to false classification. Finally, as dispersion is particularly strong in the mid-frequency regime of relevance to buried mine sonars, the results presented in the previous study and here suggest very strongly that the sound speed be estimated *in situ* at the relevant sonar frequencies, preferably through the sonar itself, rather than indirectly through core measurements.

The frequency variation of sediment sound speed and critical angle is investigated through the analysis of *in situ* acoustic measurements, and compared to core measurements and theory. As will be demonstrated, simulation using Biot theory [2], taking into account sediment porosity and permeability, suggests significant sediment sound speed dispersion in the range 1-100 kHz for the type of sand found near Elba Island. On the other hand, the study shows that for frequencies in the 2-20 kHz regime, the *in situ* critical angle estimation together with classical transmission theory adequate describe sediment penetration thus eliminating the need for estimating the 13 sediment parameters necessary for describing the sediment using Biot

theory.

Section II describes the experimental configuration and the equipment, including the characteristics of the parametric sonar used as the transmitting source, the specially designed rail [4] and the geometry of the buried hydrophone array. The results of the sediment core analysis are presented followed by estimates of the associated frequency dispersion predicted by Biot theory. Section III describes the experimental results and the analysis. The temporal characteristics of the buried hydrophone data are discussed. The results of the penetration analysis are then presented. The analysis confirms the earlier result [1], that the subcritical penetration is dominated by the evanescent field below 5-7 kHz, while scattering due to surface roughness is the dominant mechanism at higher frequencies. The low sediment speed required to theoretically explain the penetration data is then confirmed by using array delay processing to achieve an independent *in situ* estimate. Finally, in Section IV the OASES wavenumber integration code is used to model the time response of the hydrophone array. It is shown that prediction using the *in situ* sound speed estimate in combination with classical acoustic theory is virtually identical to the results achieved using full Biot theory sediment representation. It is also demonstrated that the new OASES-3D model of three-dimensional seabed scattering provides excellent prediction of the contribution above 5 kHz of the rough seabed scattering.

2
EXPERIMENTAL SETUP

2.1 Equipment and geometry

The parametric sonar used for this experiment was the SIMRAD TOPAS (TOpographic PArametric Sonar). It covers the frequency range 2-16 kHz for the secondary frequency and the 35-45 kHz for the primary frequency [1].

A single short pulse is obtained by transmitting a weighted HF-burst at the primary frequency. The TOPAS transducer consists of 24 staves, electronically controlled to form a beam in a selected direction.

The transmitting source level is approximately 238 dB for the primary frequency. The source levels obtained at different frequencies vary from about 190 to 207 dB ref. μPascal at 1 m in the 2 to 16 kHz frequency band.

In order to acquire data from various source-receiver geometries, the transmitter was mounted on a 10 m tower which in turn was mounted on a 24 m linear rail on the bottom, along which its position could be precisely controlled. The TOPAS transmitter was mounted in a Pan-and-Tilt assembly with a MRU (Motion Reference Unit) so that the transmission direction could be accurately measured, (Fig. 1).

Fig. 2 shows a picture of the portable rail facility designed at the Centre.

The rail is not horizontal. The slope is important as it modifies the grazing angles and was measured by divers who also measured the water depth along the rail, as well as over the buried hydrophone field every 10 cm.

A detailed description of the experimental set-up may be found in [1] and [4].

In order to validate the results obtained in [1] on subcritical penetration into the sediment, an array of 14 buried hydrophones was positioned in the seabed, were mounted on 5 vertical poles (Fig. 3). The burial depths of the hydrophones varied from 5 cm to 52 cm. The central pole had a hydrophone mounted above the seabed to measure the incident field.

As all positions of the source tower, the range to the hydrophone array was greater

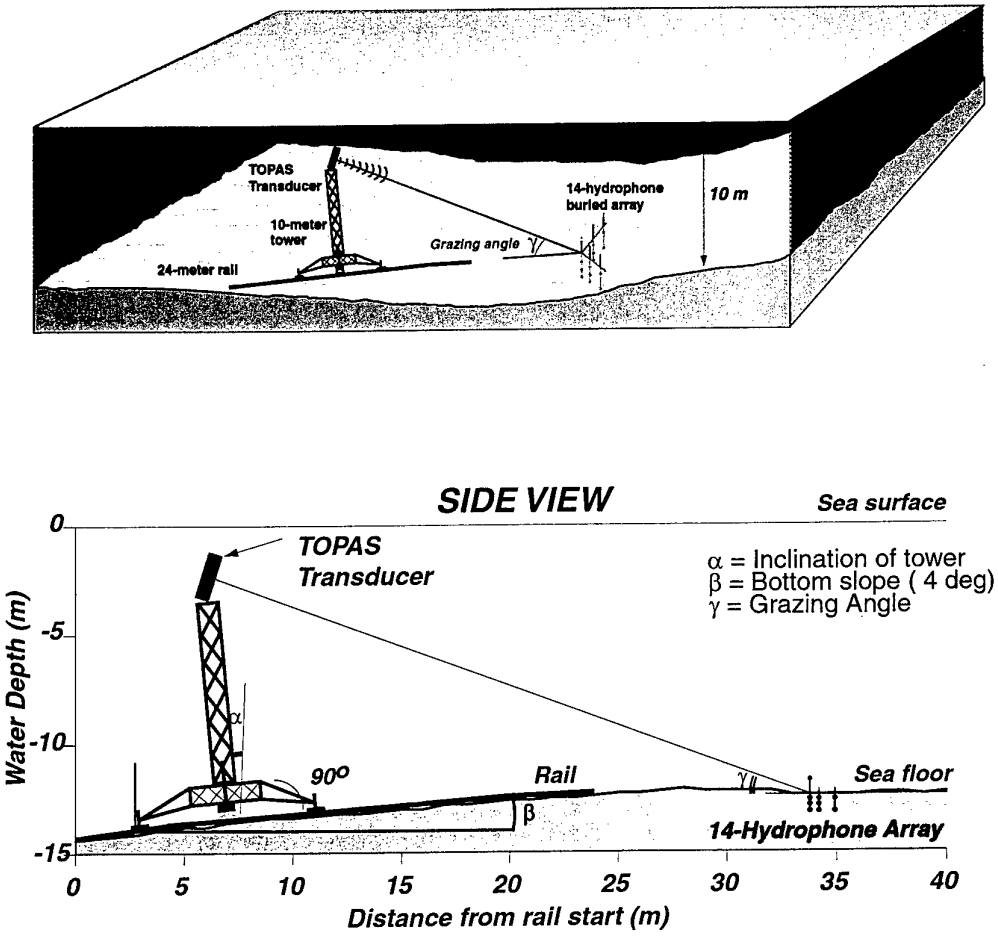

Figure 1 *Experimental configuration*

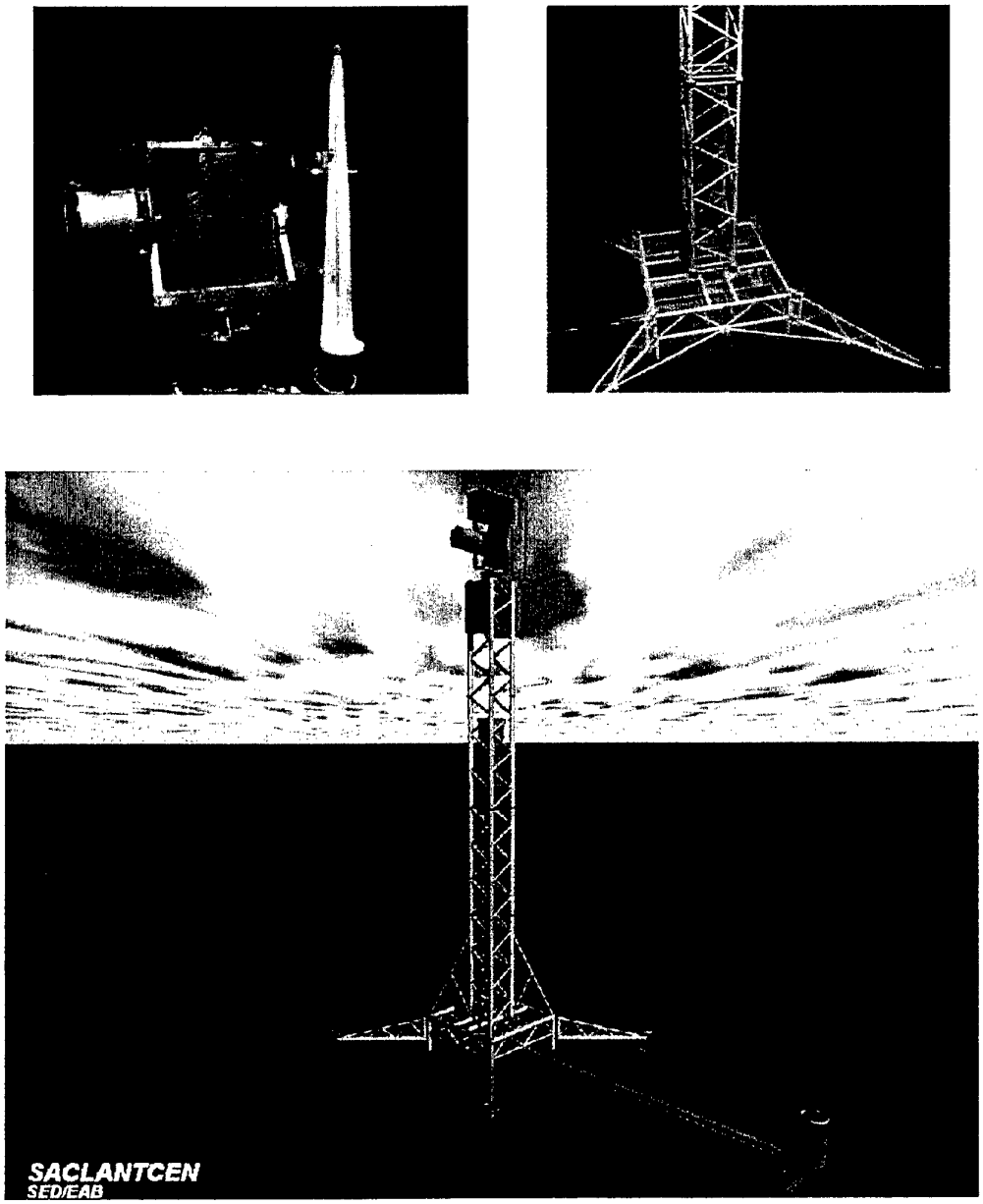

Figure 2 *Underwater portable rail facility: 24 m linear rail. 10 m tower.*

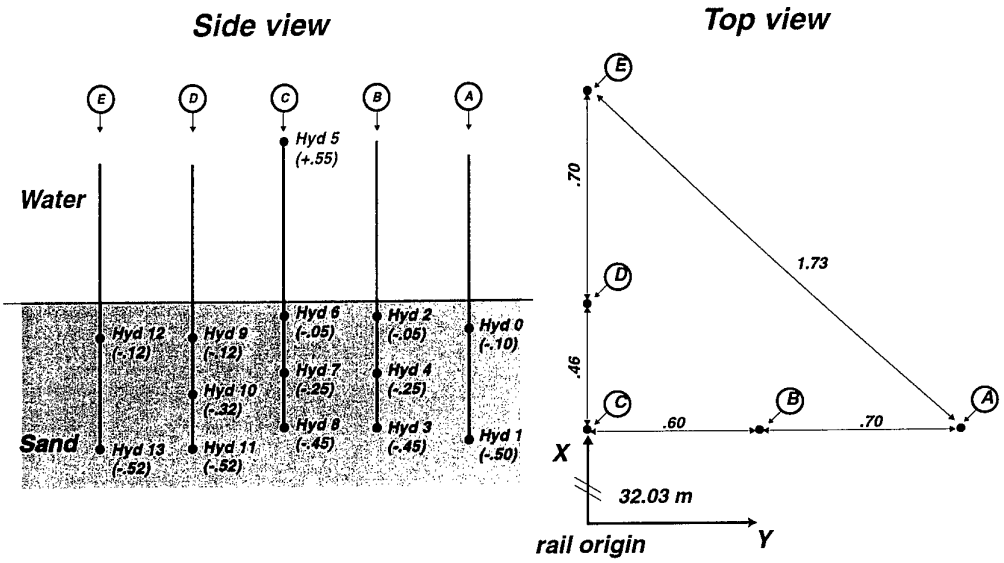

Figure 3 *14-hydrophone Reson TC4034 array geometry. The array is divided into 5 vertical poles A,B,C,D and E. The x-coordinate gives horizontal distance between rail end and each hydrophone. The y-coordinate gives distance between the rail axis and the hydrophone. The z-coordinate (depth) is given for each hydrophone in the section*

than the non-linear interaction length for the parametric sonar, such that non-linear penetration effects can be ignored in the analysis [7]. For each selected position of the source tower, the pan and tilt of the sonar was remotely adjusted to yield maximum signal at the uppermost buried hydrophone on the central pole (hydrophone number 6 in Fig. 3). A series of 100 pings were transmitted in each configuration, allowing for robustly averaged penetration measurements.

2.2 Bottom properties

The experiment was performed on a sandy bottom at 13-14 m depth near Marciana Marina on the north of Elba Island, Italy. The experiment site was selected because a sub-bottom profiling ("boomer") survey indicated the presence of a 9 m thick layer of homogeneous sediment. The seabed was characterized by a distinct ripple pattern with RMS roughness 1.5 cm, cross-ripple correlation length 25 cm, and skew angle 40° relative to the source-receiver axis.

These ripple parameters were estimated by divers, but the associated roughness spectral characteristics were estimated by stereo photography. An example of an underwater video image of the seabed is shown in Fig. 4. The digital stereo photogrammetry system uses two spatially separated cameras mounted in a rigid frame to take digital photographs of a 650 mm x 450 mm patch of the seabed. A height field is then produced via a stereo-correlation procedure [8], yielding horizontal and vertical resolutions of 1 and 2 mm, respectively. Fig. 5 shows an example of the two digital images and the associated roughness estimates.

The sediment properties were determined by core analysis (Fig. 6). Grain size estimates classified the sediment as medium sand, with average density 2.67 g/cm^3 and porosity 45.8 %. The average sound speed in the upper 25 cm of sediment was estimated to 1720 m/s by pulsed travel time measurements centered at 200 kHz. CTD measurements during the experiment indicated a well mixed water column with a sound speed of 1515 m/s. The nominal critical angle corresponding to these sound speed estimates is approximately 28°.

The permeability of the sand was estimated to be 1.7×10^{-11} m^2. The technique used was the standard method for measurement of hydraulic conductivity of saturated porous materials using a flexible wall permeameter. This technique is described in method D5084-90 (American Society for Testing and Materials). The measurements were performed at the Geology Department of the Engineering University in Rome, Italy.

The frequency variation of the sound speed predicted by Biot's theory using the measured sediment parameters is shown in Fig. 7, suggesting a sediment sound speed at low frequencies which is significantly lower than the 1720 m/s measured on the

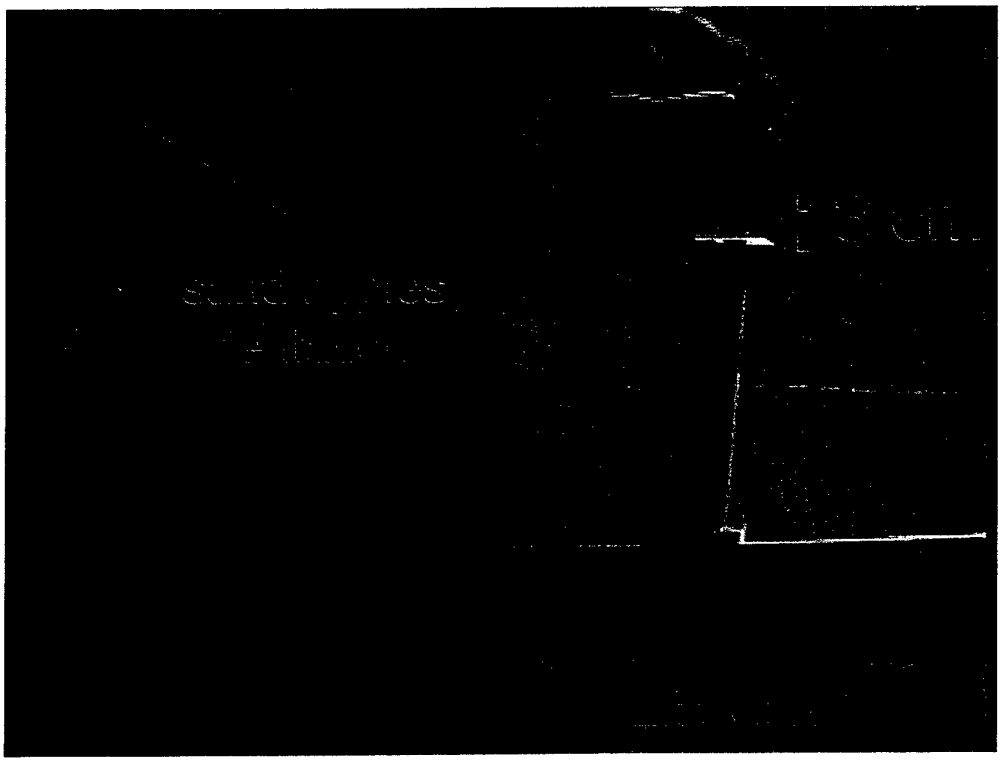

Figure 4 *Bottom roughness measured by divers with underwater digital video camera. The rms height of the ripples is measured of the order of 1.5 cm. The wavelength of the ripples is measured of the order of 25 cm. The directions of the sand ripples are not uniform everywhere, as indicated.*

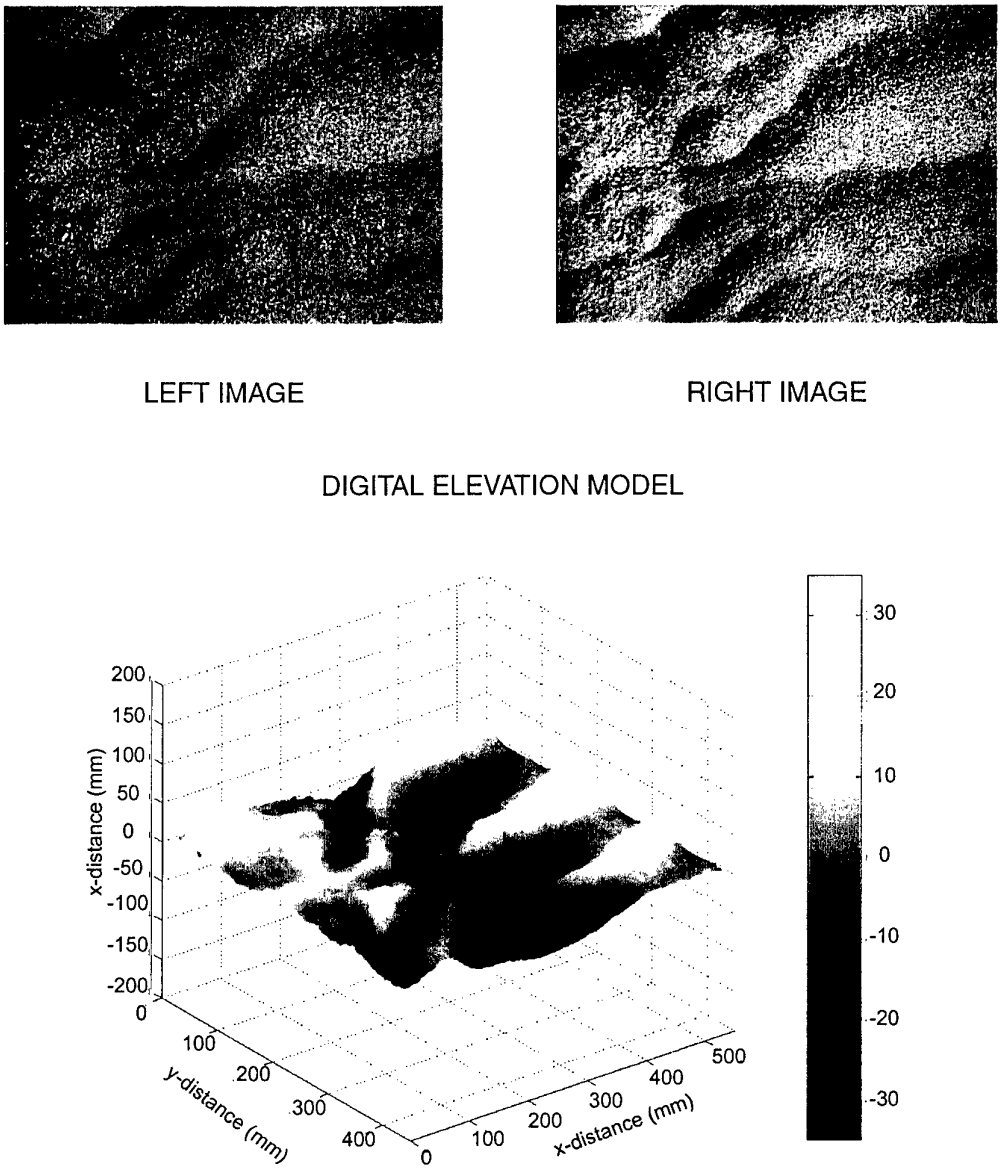

Figure 5 *Digital close-range stereo photogrammetry of the seabed. The left and right images of the bottom are shown above. The lower graph shows the estimated roughness elevation, with the colour scale representing the elevation in mm.*

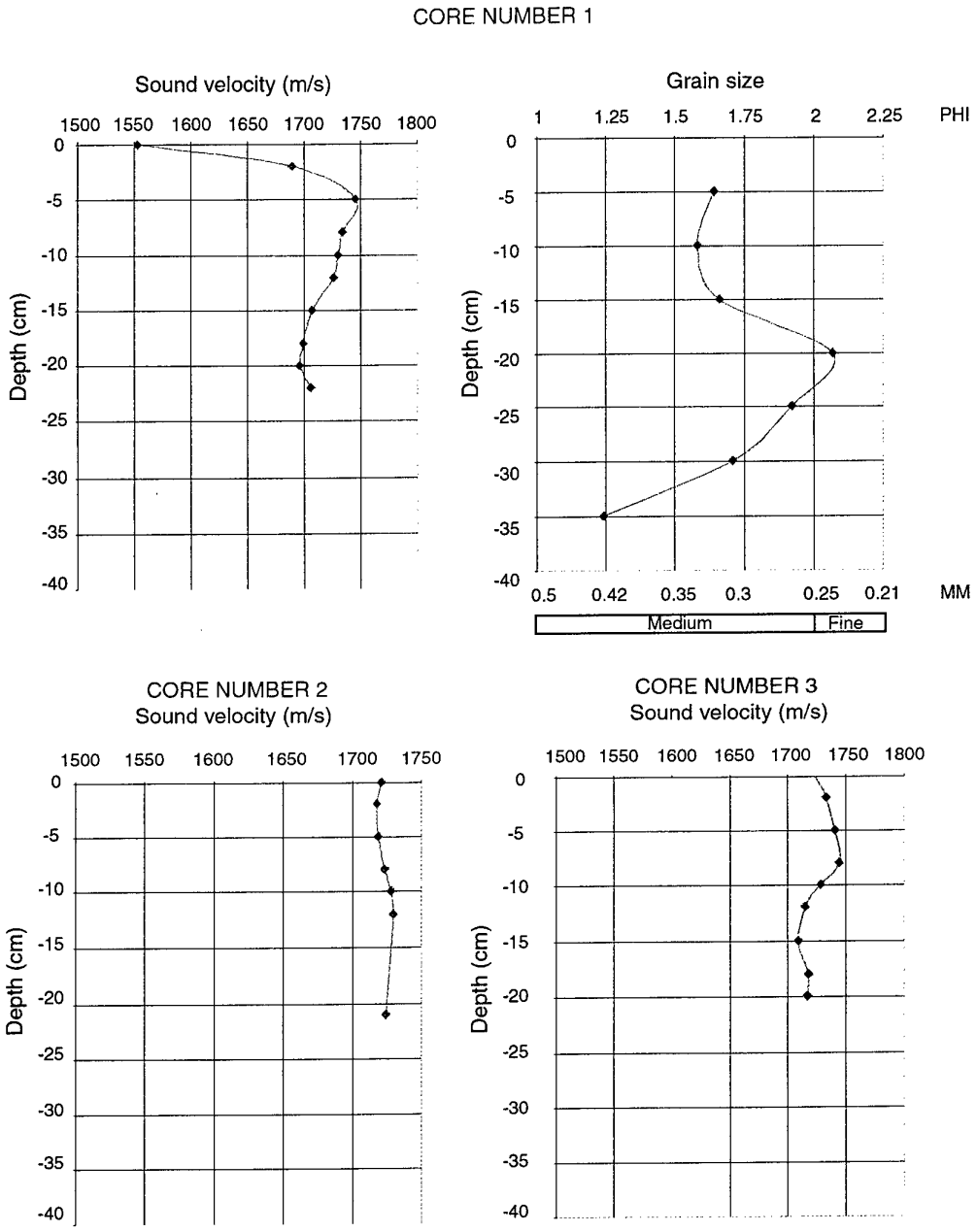

Figure 6 *Sound speed and grain size estimations measured from three different cores performed during the experiment*

cores. For example, Fig. 7 suggests a sediment sound speed 1620 m/s to 1660 m/s in the 2–16 kHz frequency bandwidth of the TOPAS sonar. The Biot parameters which were not directly measured, such as the frame bulk modulus, were chosen to be consistent with historical data for sand [2], but also to ensure that the predicted sound speed at 200 kHz was close (1710 m/s) to 1720 m/s. The parameters used for the Biot model are given in Table 1.

Table 1 *Biot parameters*

Fluid density (kg/m^3)	1000
Bulk modulus of pore fluid (Pa)	2.27E09
Viscosity of pore fluid ($kg/(m/s)$)	1E-03
Grain density (kg/m^3)	2650
Bulk modulus of grain (Pa)	3.6E10
Porosity of sand	.43
Permeability of sand (m^2)	1.7E-11
Pore size coefficient (m)	5E-05
Shear modulus of sediment frame (Pa)	2.61E07
Bulk modulus of sediment frame (Pa)	4.36E07
Shear attenuation of sediment frame (dB/*lambda*)	1.3
Bulk attenuation of sediment frame (dB/*lambda*)	1.3
Virtual mass parameter	1.25

The frequency dispersion for porous sand is greatest in the mid-frequency regime where the sound speed transitions from its low-frequency to its high-frequency limits. The characteristics of this transition regime are particularly sensitive to sediment permeability, Stoll [2] illustrated in Fig. 7. The dashed-dotted curve shows the dispersion predicted using the measured permeability of 1.7×10^{-11} m^2, while the other curves show the predictions for permeabilities of 10^{-9}, 10^{-10}, and 10^{-11} m^2, with all other parameters fixed. The center frequency as well as the width of the transition region is clearly extremely sensitive to the permeability.

It should be stressed that the sediment parameters, both measured and historical are associated with significant uncertainty and the sound speed dispersion estimates in Fig. 7 should not be used quantitatively. They do show that within the Biot theory framework, dispersion on the order of 100 m/s is realistic and consistent with the *in situ* critical angle estimates described in the following.

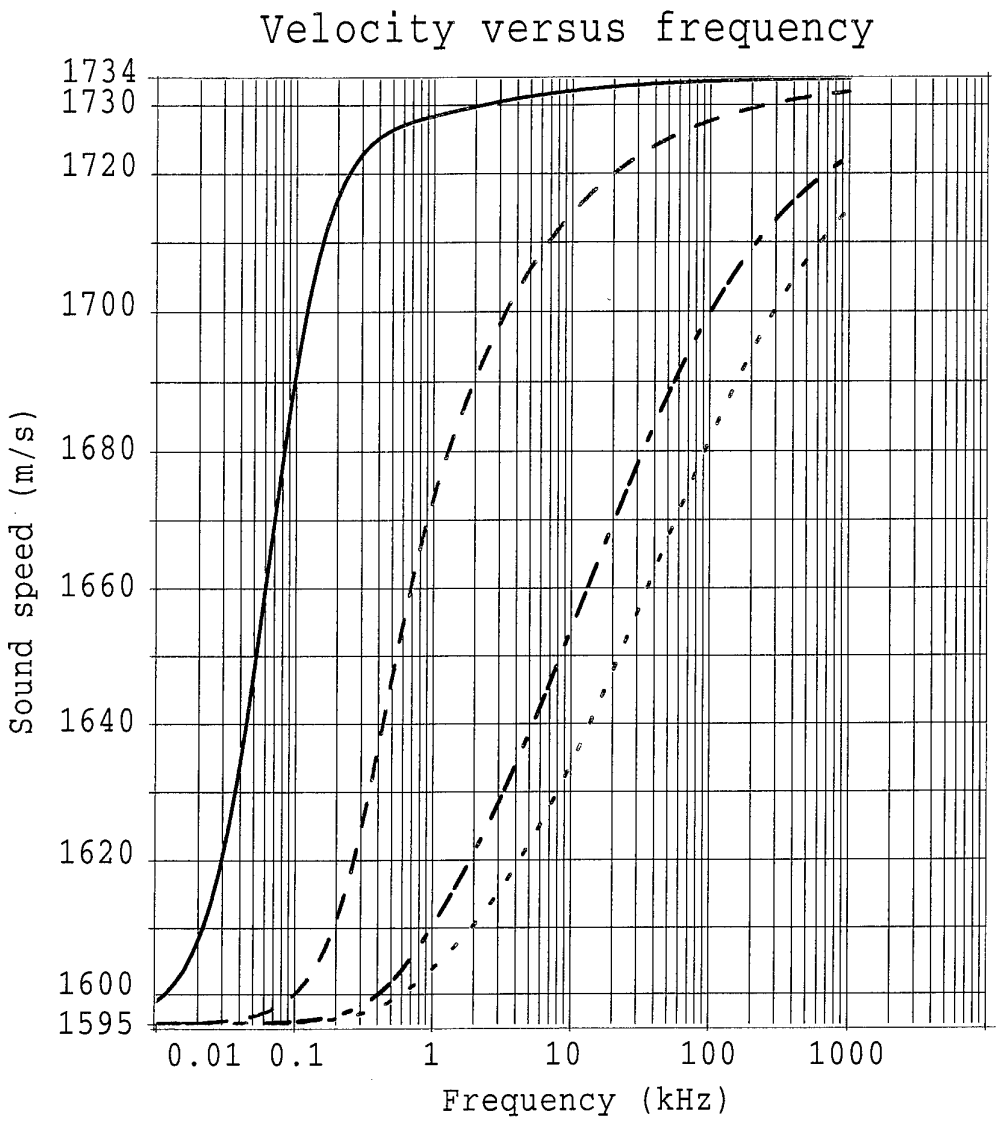

Figure 7 *Frequency dispersion of sound speed in sand as predicted by Biot theory. Four different values of permeability are considered: Solid Line:* 10^{-9} m^2, *dashed line:* 10^{-10} m^2, *dot-dashed line:* 1.7×10^{-11} m^2, *dotted line:* 10^{-11} m^2.

3

Results and Analysis

3.1 Hydrophone Signals

Signals were recorded on the array for 16 different positions of the TOPAS transmitter at grazing angles from 13.5° to 31.5° in steps of one degree. Figure 8 shows examples of the signals received on the 14 hydrophones at grazing angles: 30°, 23°, 16°, an 13.5°. The nominal critical angle is 28° if the sediment is assumed to have a sound speed of 1720 m/s as measured on the cores. The first angle is nominally supercritical, the remaining three are subcritical. The results in Fig. 8 do not reflect amplitude variations as automatic scaling was applied to each hydrophone. However, the results demonstrate clearly the qualitative differences in the penetration above and below critical, with the subcritical penetration showing a significant decrease in correlation with depth of the hydrophone, suggesting the importance of seabed scattering mechanisms in this angular regime. Hydrophone number 1 which was buried at a depth of 50 cm was defective. Hydrophone number 5 was located 55 cm above the seabed and shows two distinct arrivals, one corresponding to the incident field, and one corresponding to the coherent reflection from the seabed. At all angles the reflected signal was sufficiently separated in time to allow windowing of the incident pulse.

Very high signal to noise ratios were achieved on all the buried hydrophones, even at subcritical grazing angles. The dotted lines in the two lower frames of Fig. 8 indicate a 'ghost' arrival associated with a strong reflection from the hydrophone cable on the bottom behind the array. However, this 'ghost' arrival does not interfere with the data we are interested in.

Fig. 9 shows the signals received by the three buried hydrophones of the central pole C (hydrophones 6–8), at grazing angles, 30°, 18°, and 13.5°. Above critical, the three hydrophone signals are highly correlated with a well defined moveout characteristic of supercritical transmission. Also, the signals are close replicas of the incident field measured above the interface.

At the other two, subcritical angles, the received signals have two distinctly different components. The first part of the signal appears relatively coherent, but with an obvious decrease in high frequency content for increased burial depth. There is no apparent moveout of this arrival with depth. As discussed later, this behaviour

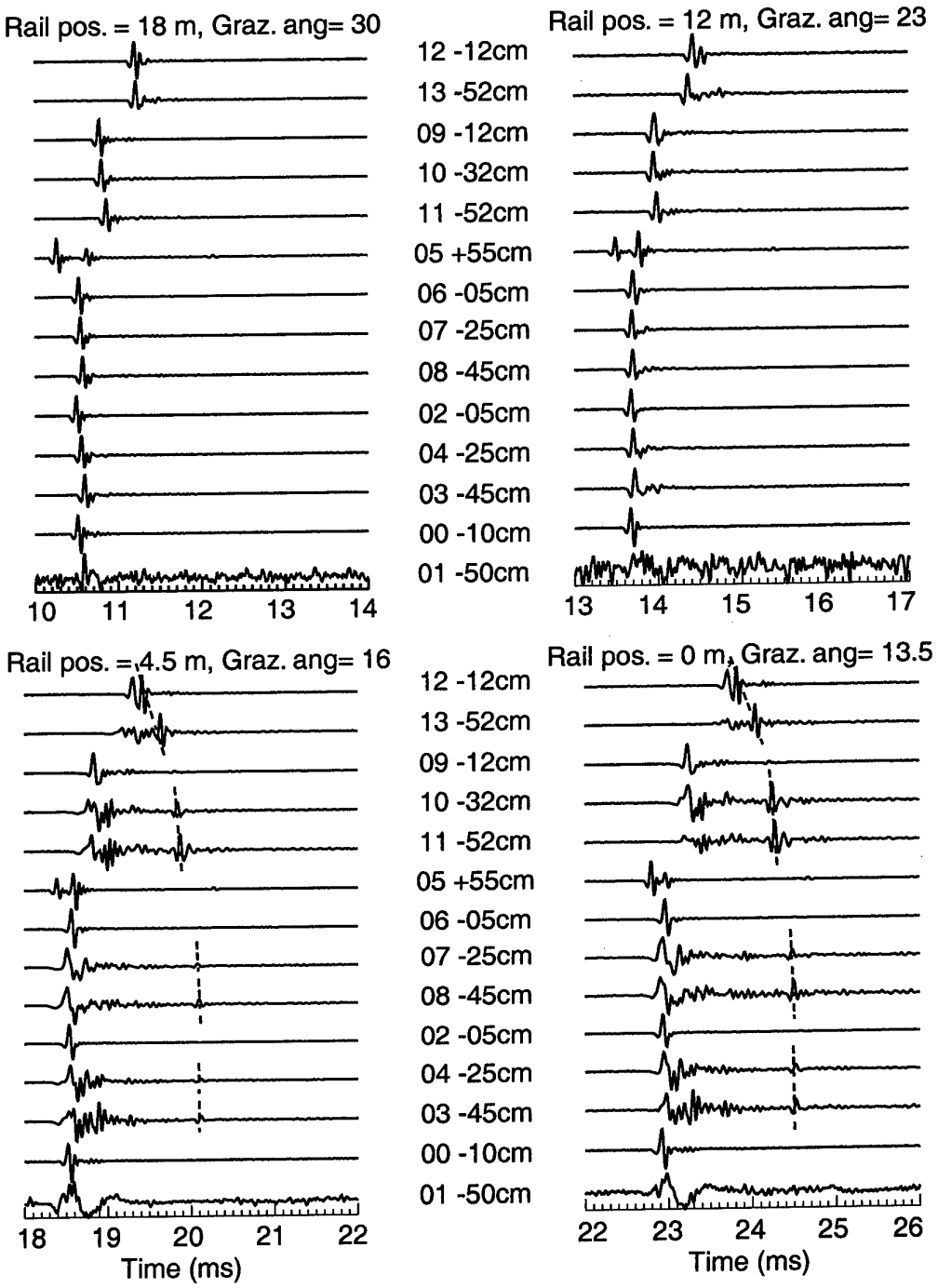

Figure 8 *Examples of signals received on buried hydrophone array for four different incident grazing angles,* 30°, 23°, 16°, *and* 13.5°.

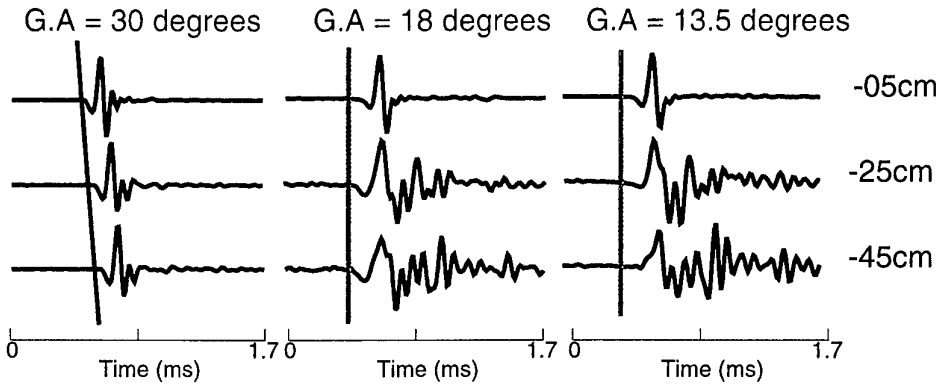

Figure 9 *Signals received on central pole (C) of the buried hydrophone array for incident grazing angles* 30°, 18°, *and* 13.5°. *Arrival moveout indicated by the lines suggests that the highest grazing angle is supercritical, while the two lower grazing angles are subcritical.*

is consistent with the prediction of classical transmission theory in the evanescent regime.

The second part of these signals appears uncorrelated between receivers and becomes increasingly dominant with depth, consistent with this signal being associated with a seabed scattering mechanism. The dominance of higher frequencies in the second part of the signal is also consistent with this interpretation [1].

The dominant feature of the signals is the difference in relative arrival time above and below critical angle (Fig. 9). Thus, at supercritical angles an increase in delay or moveout is observed with depth, consistent with the classical theoretical prediction of the transmitted field being refracted into the bottom at these angles [6].

Below critical incidence, classical theory predicts the transmitted field to be an horizontally propagating *lateral wave* with evanescent amplitude distribution in depth [6]. It will therefore manifest itself as having no moveout with depth, clearly reflected in the initial coherent component at the two subcritical angles in Fig. 9.

This fundamental difference in the temporal characteristics of the penetrated field is a robust indicator of the effective *critical angle* for the sediment and may therefore be used for estimating sediment sound speed. It will be demonstrated that the sound speed estimates obtained using this approach are consistent with the effective sound

speeds required to theoretically match the frequency and grazing angle dependence of the observed amplitude distribution in the sediment.

3.2 Bottom Penetration Analysis

To quantify the acoustic penetration into the sediment a measure called the *"penetration ratio"* was devised [1]. For a given frequency, the penetration ratio is defined as the magnitude squared of the ratio of the pressure at a point in the sediment to a reference pressure,

$$PR(f,z) = \left|\frac{P(f,z)}{P_{ref}(f)}\right|^2 = \frac{|P(f,z)|^2}{|P_{ref}(f)|^2}. \tag{1}$$

The reference pressure is defined as the pressure amplitude of the incident field at the seabed, i.e. pressure that would exist at the seabed in the absence of the sediment. Thus, the penetration ratio directly corresponds to the pressure produced by a unit amplitude incident wave field. To achieve this, the reference pressure is here chosen as the frequency spectrum of the time-gated reference signal on the hydrophone in the water. Note that the definition allows the penetration ratio to be larger than unity, or positive in terms of dB, because of the effect of the reflected wave.

For an incident plane wave of time dependence $\exp(-j2\pi ft)$ and unit pressure amplitude, the penetrated signal is, according to classical theory [5, 6].

$$P(f,z) = \frac{2m\sin\theta}{m\sin\theta + \sqrt{n^2 - \cos^2\theta}} \exp\left[jkx\cos\theta + jk\sqrt{n^2 - \cos^2\theta}z\right]. \tag{2}$$

Here, with the water being the reference, $m = \rho_1/\rho$ is the sediment density ratio, $n = c/c_1$ is the normalized index of refraction of the sediment, and θ is the incident grazing angle. Attenuation in the bottom is taken into account by making the index of refraction complex, $n = n_r(1 + j\delta)$, where δ is the *loss tangent*, which relates to the the *attenuation coefficient* α in dB/λ, as $\alpha = 54.58\delta$ [6].

At subcritical incidence, $\cos\theta > n$, the bottom field becomes evanescent, decreasing exponentially (i.e. linearly in dB) with frequency, burial depth and grazing angle,

$$P(f,z) = \frac{2m\sin\theta}{m\sin\theta + j\sqrt{\cos^2\theta - n^2}} \exp\left[jkx\cos\theta - k\sqrt{\cos^2\theta - n^2}z\right]. \tag{3}$$

Fig. 10 shows the estimated penetration ratio in dB at the buried hydrophones on the central pole C, for a series of grazing angles between 13.5° and 30°. For all three burial depths the highest grazing angle results show a quasi-linear decrease

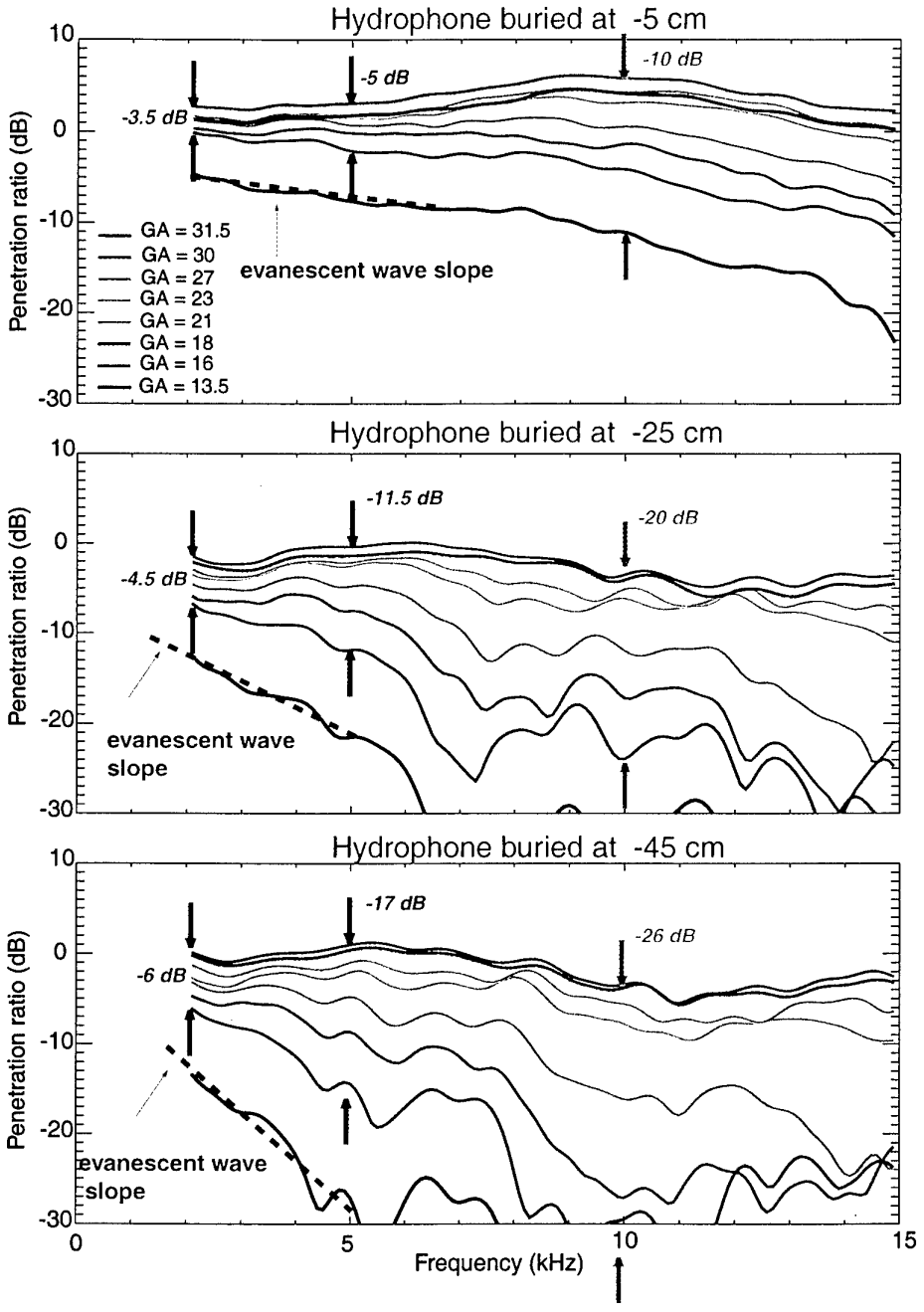

Figure 10 *Penetration ratio in dB versus grazing angles for hydrophones on central pole (C), buried at 5, 25, and 45 cm depth. The results for eight different grazing angles in the range* 31.5° *(red curves) to* 13.5° *(black curves) are shown.*

with frequency which is in agreement with Eq. (2) assuming a bottom attenuation of $\alpha = 0.5$ dB/λ.

At the lowest grazing angles in particular, the penetration ratio is strongly dependent on frequency. For frequencies up to 5-7 kHz the penetration ratio (expressed in dB) is decreasing quasi-linearly with frequency, with the slope increasing with the burial depth and grazing angle. As indicated by the dashed lines, this behavior is consistent with the subcritical prediction of classical penetration theory. The lines correspond to the result of Eq. (3) assuming a sound speed of 1626 m/s in the sediment.

As expected, the results in Fig. 10 have a distinct interference pattern where seabed scattering is the dominant mechanism, i.e. above approximately 5 kHz, and at low grazing angles. However, the interference patterns at different grazing angles are clearly correlated, even though the results are obtained following rearrangement of the source tower. In fact, as the grazing angle decreases, the interference pattern shifts down in frequency consistent with the Bragg scattering condition. Thus, the Bragg theory predicts interference minima at a frequency which depends on the water sound speed c, the roughness correlation length L in the insonification direction, and the incident grazing angle:

$$f \simeq \frac{c}{L \cos\theta} \tag{4}$$

Detailed analysis confirms that the frequency and angle dependency of the interference patterns are consistent with Eq. (4). This strongly supports the hypothesis of the seabed roughness being the dominant subcritical penetration mechanism at high frequencies [9],[10].

The analysis of the penetration ratio strongly supports the conclusion of earlier work [1], using a different data set, that the subcritical penetration is dominated by the evanescent field below 5-7 kHz, while scattering due to surface roughness is the dominant mechanism for higher frequencies. These results also confirm the earlier finding that the significant dispersion predicted by Biot theory for porous sand must be accounted for to match the data theoretically. In the following section an independent estimate of the sediment sound speed is achieved, using array processing on the buried hydrophone array.

3.3 Sound speed estimation

To confirm the hypothesis that frequency dispersion of sandy sediments must be taken into account when interpreting bottom penetration data in the 2-20 kHz regime, a more direct measurement of sound speed was devised.

The bandwidth of the source signal allows for time of arrival estimates for the coherent component of the signal on the order of 0.05 ms, which however is only

slightly less than the 0.1 ms order of the travel time between pairs of hydrophones in the array. This, together with the uncertainty of the array element positions of order cm makes it impossible to use correlation analysis to estimate the sediment sound speed. However, as it will be demonstrated, the grazing angle dependence of the arrival time structure in depth can be used to robustly estimate the effective critical angle, which can then in turn be translated into an effective sound speed for the sediment. This *in situ* estimate has the advantage of being representative for the bottom at the actual sonar frequencies, which is particularly important for highly dispersive sediments such as porous sand.

In the following section, it will be shown that the sound speed estimates are consistent with Biot theory predictions of the full time domain array response, using measured sediment parameters such as porosity, grain size and permeability, in combination with historical parameter values for this type of sand.

The variation of the time of arrival between hydrophones at different burial depths on the same pole is first estimated as a function of grazing angle. These delays are then compared to the theoretical delays derived from the standard reflection theory in discretely layered fluids described in Eqs. (2) and (3).

The analysis will be performed using the hydrophones on the central pole C. To evaluate the frequency variation of the depth-dependent arrival delay, the analysis is performed in the frequency domain in terms of phase difference.

Figure 11 shows the phase shift variations *versus* frequency obtained for four different grazing angles. At 31.5° grazing angle, the results are consistent with the theory for a plane interface. The phase shifts (solid curve) measured between the hydrophones buried at 5 cm and 25 cm are identical to those (dash-dotted curve) measured between the hydrophones buried at 25 cm and 45 cm. Moreover, the phase shifts (dashed line) measured between the hydrophones buried at 5 cm and 45 cm are twice the delay between the close neighbours, as expected. The close to linear frequency dependence is evidence of the high coherence of the penetrated signal above critical incidence.

The phase shifts clearly decrease with decreasing grazing angle and continue to be nearly linear in frequency even at the lowest grazing angles, at least below 5 kHz where the evanescent coupling is dominant. At the higher frequencies, the phase shifts fluctuate, again suggesting a scattering mechanism being responsible for the penetration. The sound speed estimation analysis was therefore restricted to the 2-5 kHz band. Within this band, it is assumed that there is no dispersion (i.e., sound speed is constant vs. frequency), and the phase shift ϕ can therefore be expressed as $2\pi f\tau$ where τ is the temporal delay. The slope of the phase shifts in Fig. 11 therefore provides an estimate of the delays.

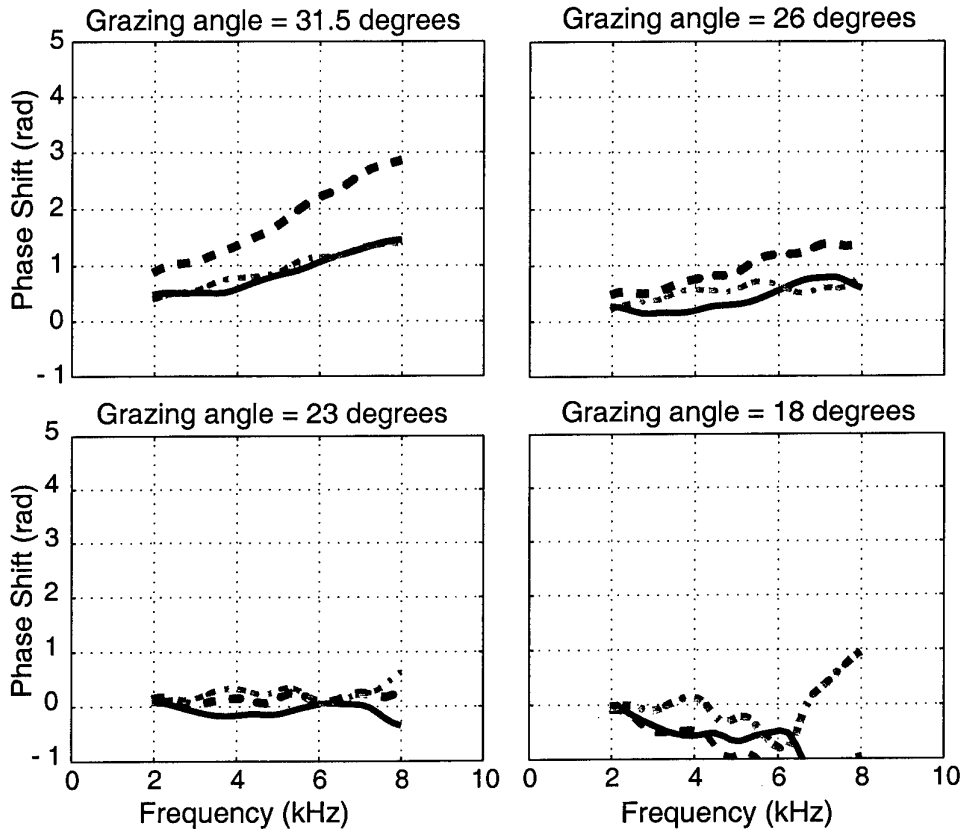

Figure 11 *Phase shift in radians versus frequency measured between two hydrophones on pole C. Solid line: Hydrophones at 5 and 25 cm depth. Dashed-dotted line: Hydrophones at 25 and 45 cm depth. Dashed line: Hydrophones at 5 and 45 cm depth.*

Using this procedure, the delays between hydrophones were estimated from the *in situ* data for all grazing angles, ranging from 13.5° to 31°, in steps of one degree. Figure 13 shows the results as function of grazing angle for the hydrophones on pole C. The estimated phase delays between the hydrophones at 5 and 25 cm depth are shown as filled circles, and the delays between 25 and 45 cm depth are shown as empty circles,

The theoretical phase delays are given by the imaginary part of the argument to the exponential function in Eq. (2). However, the poles with the buried hydrophones were not vertical as (Fig. 12), and the projected tilt angle θ_t must be taken into account. Thus, for two hydrophones separated by distance z along the pole, the associated coordinate separations are $(\Delta x, \Delta z) = (zsin\theta_t, z\cos\theta_t)$. Consequently, the theoretical delay between the two hydrophones is

$$\tau_{ab} = \frac{1}{2\pi f}\mathrm{Re}\left[kz(\sin\theta_t\cos\theta + \cos\theta_t\sqrt{n^2-\cos^2\theta})\right] \quad (5)$$

Note that the index of refraction n is complex due to the attenuation, which was assumed to be 0.5 dB/λ, as estimated above in connection with the penetration ratio analysis. This value is typical for a sandy sediment [6].

The theoretical predictions that best match the data are indicated by the solid and dashed curves respectively in Fig. 13. The delays for both hydrophone pairs are best matched assuming a sediment sound speed of 1626 m/s. However, the tilt angle giving the best match was $-10°$ for the two upper hydrophones and $-3°$ for the two lower hydrophones. This difference is not unreasonable given that the pole was flexible and deployed by divers.

The experimental estimates and the theoretical match indicate a distinct change in slope, or 'elbow', of the delay curves at the critical angle, separating a region with constant delay corresponding to the evanescent penetration regime and the super-critical regime where the penetrated field is propagating vertically and is therefore associated with an increasing phase delay for increasing incident grazing angles. Based on the scattering of the experimental results around the theoretical prediction, the standard deviation of the position of the 'elbow' and therefore the critical angle estimate, is approximately one degree. In terms of sound speed estimate, this corresponds to a resolution of order 10 m/s, which is significantly better than that which can be achieved by correlation analysis between array elements.

The robustness of using the grazing angle dependence of the phase delays to estimate sediment speed is illustrated in Fig. 14. Here the data and theoretical match for one of the hydrophone pairs are compared to the theoretical prediction achieved using a sediment sound speed of 1720 m/s as estimated from the core measurements. This comparison makes it evident that the high-frequency core measurements of sediment speed lead to a heavily over-estimated critical angle at lower frequencies, suggesting

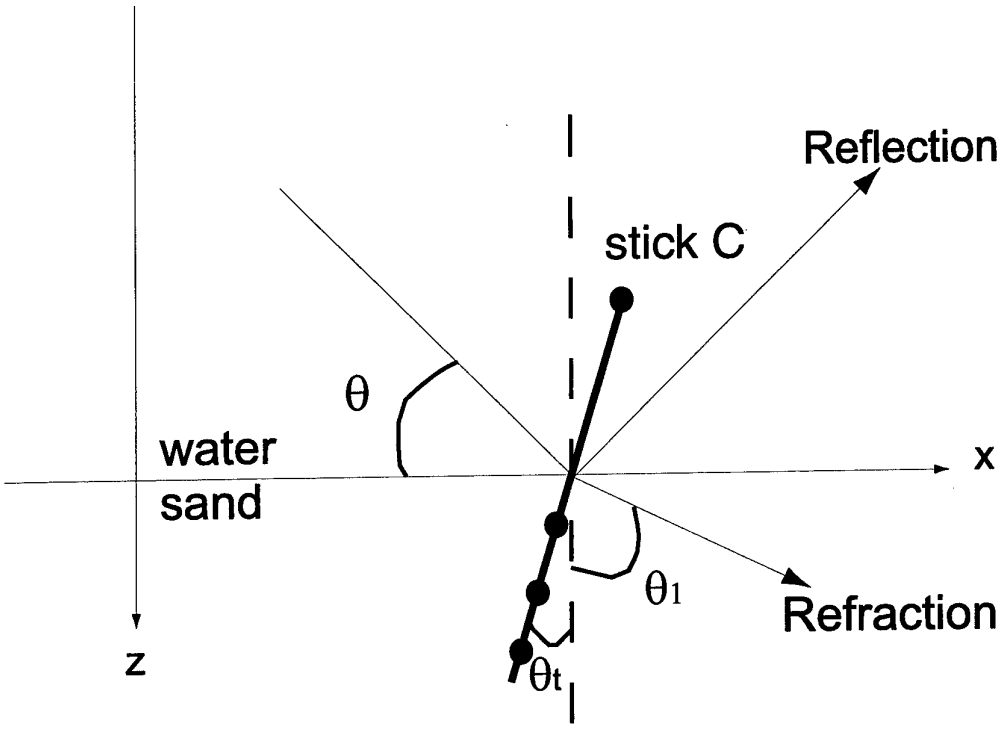

Figure 12 *Reflection and transmission geometry for tilted hydrophone pole.*

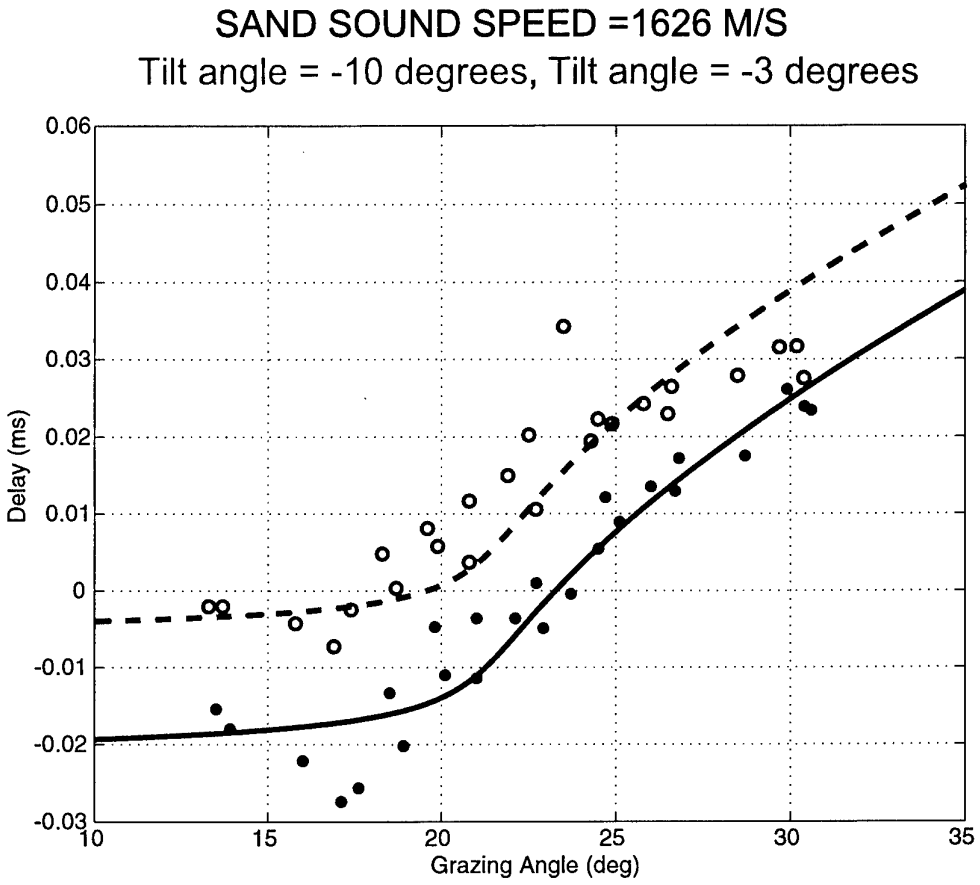

Figure 13 *In situ critical angle and sound speed estimation. Comparison of measured and predicted phase delays as a function of grazing angle. Filled and empty circles indicate the measured delays between the hydrophones at 5 and 25 cm, and the hydrophones at 25 and 45 cm, respectively. The solid and dashed lines represent theoretical predictions providing the best match to the data, both assuming a sound speed of 1626 m/s, but different tilt angles of* $-10°$ *and* $-3°$*, respectively.*

very strongly that dispersion be accounted for in sandy sediments. As indicated in Fig. 7 the Biot theory predicts a sediment sound speed 1610 – 1650 m/s in the 1–10 kHz frequency regime if the sound speed at 200 kHz is 1710 m/s, and the permeability is 1.7×10^{-11} m^2 as measured.

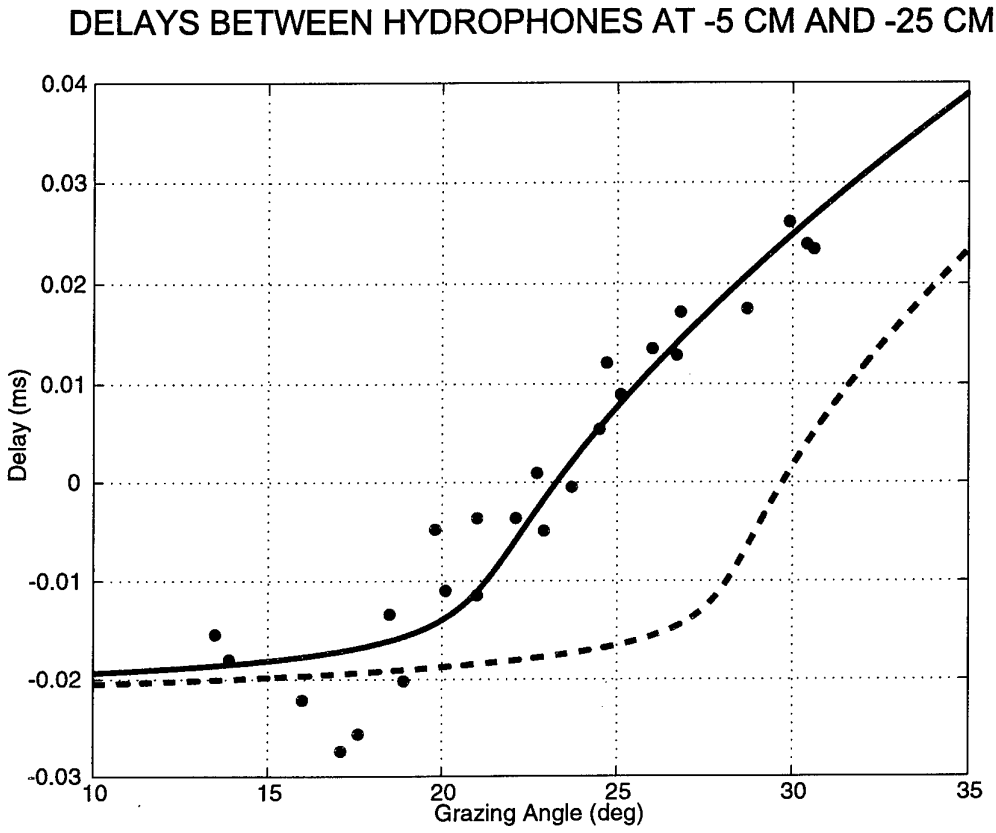

Figure 14 *Comparison of measured and predicted delays with the prediction obtained assuming the sand to be non-dispersive with a sound speed of 1720 m/s as measured at 200 kHz.*

Even though the present analysis suggests that Biot theory is needed to represent the strong frequency dispersion of sandy sediments, it is highly desirable to use a simpler acoustic-elastic representation of the sediment, with its more limited requirements in terms of environmental characterization. In the following section it will be shown that the experimental penetration results in the 2-16 kHz regime are consistently and accurately modeled by both full Biot theory and by classical acoustic theory using the in situ critical angle and sound speed estimates, thus eliminating the need for extremely involved laboratory procedures for sediment characterization.

4

OASES Time series modelling

The OASES wavenumber integration code [11] is well established for modelling seismo-acoustic propagation in arbitrary stratifications involving fluid, elastic, and poro-elastic layers or halfspaces, and is capable of directly modelling the experimental scenario of the previously described experiment.

The standard OASES model computes the field, assuming all interfaces to be plane, and is therefore applied to directly compute the coherent component of the bottom-penetrated field. Even though the model is capable of modelling arbitrary source beam patterns, the source field will here be assumed to be a plane wave, incident on the bottom at the nominal grazing angle. The impulse responses computed by OASES are then convolved with the incident field as measured by the hydrophone above the seabed.

As suggested by the analysis above, the scattering due to seabed roughness is a significant contributor to the penetration at higher frequencies. It was demonstrated in the earlier study [1] that the new OASES-3D code for modelling 3-D scattering from rough interface patches in a stratified seabed [12] accurately predicts the energy levels of the scattering component. This code will be used here to directly model the temporal response of the buried hydrophones to the scattered field.

To isolate the seabed penetration effect, the sea surface and deeper sub-bottom interfaces are ignored in the modelling. Figure 15 shows the OASES predictions of the signals on the three buried hydrophones at 5, 25, and 45 cm depth for 13.5°, 18° and 30° grazing incidence. The qualitative agreeement between the coherent part of the simulated signals and the experimental results in Fig. 9 is obviously very good. The quantitative agreement in the depth dependence of the signal amplitudes of the coherent component is evident from Fig. 10, where the theoretical results are obtained using the same classical formulation for the penetration as used by OASES. The coherent component was calculated using a fluid representation of the sediment, with sound speed 1626 m/s, as suggested by the *in situ* estimate. The scattering field was computed deterministically using modeled realizations of a seabed with given estimated roughness statistics [10], i.e. ripples with 25 cm correlation length, 40° aspect, and 1.5 cm rms height. The scattered field obviously cannot be expected to be modeled correctly deterministically, although the spatial and temporal characteristics of the experimental data are clearly captured accurately

by the model.

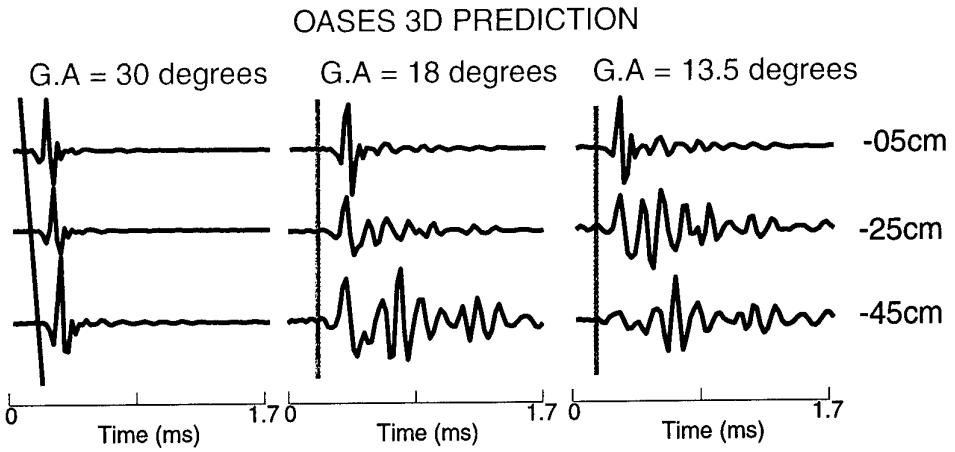

Figure 15 *OASES prediction of signals received on the central pole with hydrophones buried at 5, 25, and 45 cm depth, for grazing incident angles of* 13.5°, 18°, *and* 30°. *The direct signal measured by the hydrophone in the water is assumed as representing an incident plane wave field. The individually normalized traces may therefore be directly compared to the corresponding experimental results in Fig. 9. The sand is represented as a fluid medium with sound speed 1626 m/s, and the roughness is a random realization of the measured roughness statistics, with a 1.5 cm rms elevation.*

The fact that OASES computes the coherent and scattered components separately allows for directly analyzing the significance of each component. Thus, Fig. 16 shows the coherent component on the three hydrophones for 18° grazing incidence as a blue curve, while the total field is indicated by the red curve. This confirms the earlier interpretation of the experimental results, concluding that the initial part of the signal is dominated by the coherent component described by classical penetration theory, while the 'tail' of the signals is associated with the seabed scattering which increasingly dominates with increase in depth and decrease in grazing angle.

Figure 16 also shows, as a green curve, the coherent prediction obtained using the full Biot representation of the sediment with the sediment parameters in Table 1. Clearly, within the band of the parametric sonar, the dispersion effect is insignificant, and the classical theory produces accurate results, both in terms of amplitude and phase of the penetrated signals. The agreement is of equal quality for the other incident angles. This agreement in turn suggests that classical theory adequately represents the penetration of sound into sandy sediments, at least within a frequency decade, provided an *in situ* sediment sound speed is used.

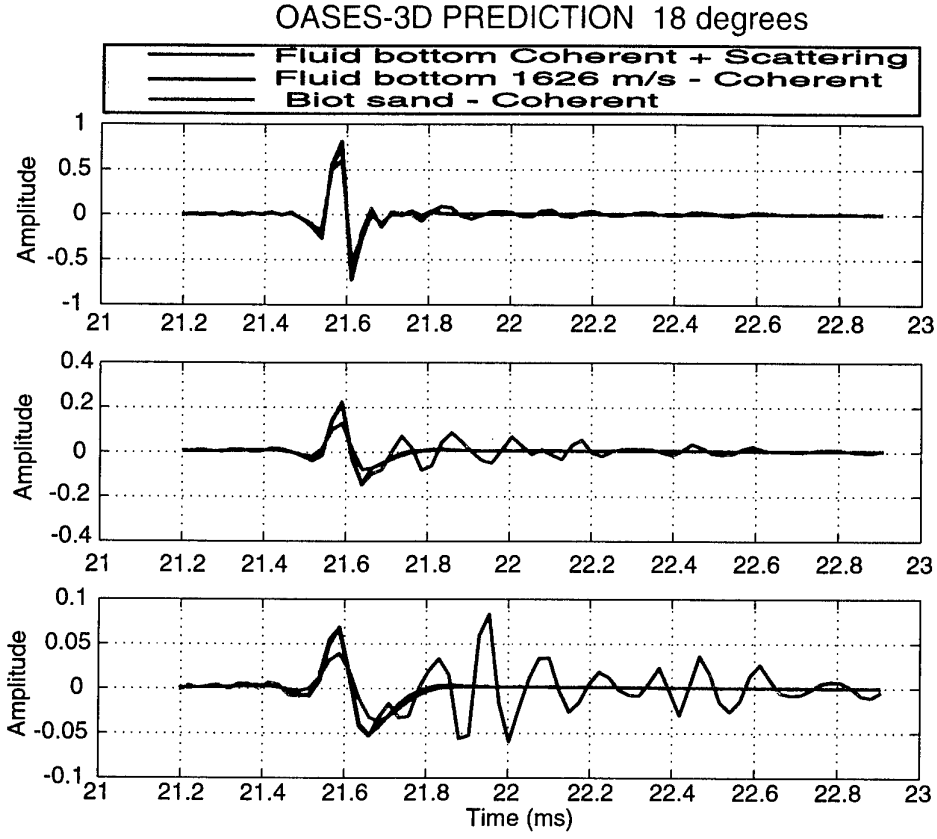

Figure 16 *OASES prediction of signals received on the central pole with hydrophones buried at 5, 25, and 45 cm depth, for grazing incident angle* 18°. *The red curve shows the full response including the scattered field, computed assuming the sand to be a fluid medium with sound speed 1626 m/s. The blue curve shows the coherent component, dominating the initial part of the penetrated signals. The green curve shows the coherent prediction when the sand is represented by Biot theory using the parameters in Table 1.*

5
CONCLUSIONS

The strong frequency dispersion of sandy sediments predicted by Biot theory and confirmed by earlier analysis of acoustic bottom penetration data was investigated by devising an independent, in situ estimation procedure for sediment sound speed. A parametric source was used to insonify a sandy seabed in the frequency range 2-16 kHz, and a buried hydrophone array was used to measure the bottom penetration over a wide range of grazing angles. It was demonstrated that the grazing angle dependence of the phase delay in the seabed provides a robust and accurate measure of the sediment critical angle, and therefore the sound speed. Consistent with earlier analysis of penetration data from other geographical areas, the present estimates of bottom sound speed confirm the presence of a significant frequency dispersion in sandy sediments, with the estimated speed at 2–5 kHz being 1626 m/s while the sound speed measurements performed at 200 kHz on core samples yielded a speed of 1720 m/s. However, as demonstrated here, this dispersion is totally consistent with the predictions of Biot theory for this type of sand. This dispersion is significant to the prediction of the sediment critical angle. On the other hand the study has shown that, within approximately a frequency decade, the experimental data are adequately modeled by classical theory provided the *in situ* sound speed estimate is used, eliminating the need for full Biot modelling with its elaborate sediment characterization. Finally, the very good agreement obtained between the experimental data and the model predictions for both the coherent and scattered contributions provide valuable validation of the OASES modelling framework, including the new 3-D seabed scattering model.

6

Acknowledgements

I would like to thank the Manning crew for their help and their constant availability during the experiment. They contributed to the success of the cruise and therefore to the quality of the data collected.

The Engineering Technology Division did a great job, not only during the cruise but also before the cruise. I would like particularly to thank: P.A. Sletner who, as Engineering coordinator, succeeded in assembling the different systems and making them work perfectly during the cruise, A. Figoli for setting up the hydrophones and the data acquisition electronics, R. Chiarabini for ensuring the good functioning of the TOPAS system, E. Michelozzi for the measurement of the cores characteristics (sound speed, grain size, permeability) and L.Gualdesi for the preparation and the deployment of the rail on the bottom.

The diving team consisting of M. Paoli and J. Staveley and divers from a company in Elba was essential for the finding of the best location of the rail, and thereafter the deployment of the rail equipment, hydrophones and cables.

I would like to thank T. Lyons who made his digital close-range stereo photogrammetry system available for the experiment and whose processing was used to give the bottom spectrum images shown in the report.

Finally, many thanks to Nick Pace, reviewer of this paper at SACLANTCEN, who, thanks to his pertinent remarks, increased its quality and readibility.

References

references in TOC (DAA, 2/97)

[1] A. Maguer, W. L. J.Fox, H. Schmidt, E. Pouliquen, E. Bovio, Mechanisms for subcritical penetration into a sandy bottom: Experimental and modeling results, submitted to *Journal of the Acoustical Society of America*

[2] R. B. Stoll, *Sediment Acoustics*, Springer-Verlag, New-York, 1989

[3] N. P. Chotiros, A. M. Mautner, A. Lovik, A. Kristensen, and O. Bergem, Acoustic penetration of a silty sand sediment in the 1-10 kHz band, *IEEE Journal of Oceanic engineering*, 22, 604-615, 1997.

[4] S. Fioravanti, A. Maguer, W. L. J. Fox, L. Gualdesi, and A. Tesei, Underwater rail facility for highly controlled experiments at sea. Submitted to Third European MAST Conference, Lisbon, Portugal, 1998.

[5] L. M. Brekhovskikh, *Waves in Layered Media.* New York: Academic Press, second ed., 1980.

[6] F. B. Jensen, W. A. Kuperman, M. Porter, H. Schmidt, *Computational Ocean Acoustics.* American Institute of Physics, AIP press, New-York, 1994

[7] D. J. Wingham, N. G. Pace, and R. V. Ceen, An experimental study of the penetration of a water-sediment interface by a parametric beam, *Journal of the Acoustical Society of America*, 79, 363-74, 1986.

[8] A. P. Lyons, T. Akal and E. Pouliquen , Measurements of sea floor roughness with close range digital photogrametry, *OCEANS 98*, Nice, September 98.

[9] E. I. Thorsos, D. R. Jackson, J. E. Moe, and K. L. Williams, Modelling of subcritical penetration into sediments due to interface roughness, in *High Frequency Acoustics in Shallow Water* (N. G. Pace, E. Pouliquen, O. Bergem, and A. P. Lyons, eds.), no. CP-45 in SACLANTCEN Conference Proceedings Series, 563-569, NATO SACLANT Undersea Research Centre, June 1997.

[10] E. Pouliquen, A. P. Lyons, N. G. Pace. Penetration of acoustic waves into sandy seafloor at low grazing angles: The Helmhotz-Kirchoff approach, SACLANTCEN SM290, NATO SACLANT Undersea Research Centre report, La Spezia, Italy, 1998.

[11] H. Schmidt, *OASES: Version 2.1. User Guide and Reference Manual.* Massachusetts Institute of Technology, 1997.

[12] H. Schmidt and J. Lee, Physics of 3D-scattering from rippled seabeds and buried targets in shallow water, *Journal of the Acoustical Society of America*, 105, 1605-1617, 1999.

Document Data Sheet

Security Classification		Project No.
UNCLASSIFIED		03-A
Document Serial No.	**Date of Issue**	**Total Pages**
SR-297	July 1999	37 pp.

Author(s)

Maguer, A., Fox, W.L.J., Schmidt, H., Bovio, E.

Title

Sediment sound speed and critical angle estimations derived from *in situ* acoustic measurements.

Abstract

Understanding the basic physics of sound penetration into ocean sediments is essential to the design of sonar systems which can detect, localize, classify and identify buried objects. The sediment sound speed is a crucial parameter as the ratio of sound speed at the water-sediment interface determines the critical angle. Sediment sound speed is typically measured from core samples using high frequency (100's of kHz) pulsed travel time measurements. Earlier work on subcritical penetration into sandy sediments has suggested that the effective sound speed in the 2-20 kHz range is significantly lower than the core measurements results. Simulation using Biot theory for propagation in porous media confirmed that sandy sediments may be highly dispersive in the range 1-100 kHz. It is shown that a direct and robust estimate of the critical angle and therefore the sediment sound speed, at lower frequencies can be achieved by analyzing the grazing angle dependence of the phase delays observed on a buried array.

A parametric source with secondary frequencies in the 2-16 kHz range was directed toward a sandy bottom similar to the one investigated in the earlier study. An array of 14 hydrophones was used to measure penetrated field. The critical angles were estimated by analyzing the variations of signal arrival times *versus* frequency, burial depth and grazing angle. Matching the results with classical transmission theory yielded a sound speed estimated in the sand of 1626 m/s in the frequency range 2-5 kHz, significantly lower than the 1720 m/s estimated from the cores at 200 kHz. The dispersion is consistent with Biot theory.

Keywords

Seafloor – scattering – sound penetration – Kirchhoff – small perturbation – evanescent wave – Biot theory

Issuing Organization

North Atlantic Treaty Organization
SACLANT Undersea Research Centre
Viale San Bartolomeo 400, 19138 La Spezia, Italy

[From N. America: SACLANTCEN (New York) APO AE 09613]

Tel: +39 0187 527 361
Fax:+39 0187 527 700

E-mail: library@saclantc.nato.int

The SACLANT Undersea Research Centre provides the Supreme Allied Commander Atlantic (SACLANT) with scientific and technical assistance under the terms of its NATO charter, which entered into force on 1 February 1963. Without prejudice to this main task - and under the policy direction of SACLANT - the Centre also renders scientific and technical assistance to the individual NATO nations.

This document is approved for public release.
Distribution is unlimited

SACLANT Undersea Research Centre
Viale San Bartolomeo 400
19138 San Bartolomeo (SP), Italy

tel: +39 0187 527 (1) or extension
fax: +39 0187 527 700

e-mail: library@saclantc.nato.int

NORTH ATLANTIC TREATY ORGANIZATION